Table I. Primers

Name	Sequence
Real-time RT-PCR	
RT-*gyrA*-f	CGACTTGTCTGAACGCCAAA
RT-*gyrA*-r	TTATCACGTTCCAAACCAGTCAA
RT-*degP*-f	CGACGGAGCTAAACGAATTGA
RT-*degP*-r	AGTATCAGCTCCAACTAATTCACCAA
RT-*scpA*-f	TGCAGCGGCAGACTCAAC
RT-*scpA*-r	TTTGACCGTAGCAGTTTCAGTGA
RT-*scpC*-f	ACACAGAATTGCTAACAGATCATGTAGA
RT-*scpC*-r	GGTACGTTTTTAAGGAGCGAGAAGT
RT-*rbfA*-f	GTCACCTCCCTCATCGAAGATT
RT-*rbfA*-r	TGTACATAGCCTTGGCCTGAAA
RT-*pepXP*-f	GACACGTCACAGCTGATTCGA
RT-*pepXP*-r	AGTTGGCCATCTTGATCGGTAT
RT-*aarA*-f	GCAACTGGTGCTCAAGCTATTT
RT-*aarA*-r	CACAACTGATCTGGCATTGCT
RT-*β-Actin*-f	GAAATCGTGCGTGACATCAAAG
RT-*β-Actin*-r	TGTAGTTTCATGGATGCCACAG
RT-*KC*-f	CTGGGATTCACCTCAAGAACATC
RT-*KC*-r	CAGGGTCAAGGCAAGCCTC
RT-*IL-6*-f	TAGTCCTTCCTACCCCAATTTCC
RT-*IL-6*-r	TTGGTCCTTAGCCACTCCTTC
RT-*IL-1β*-f	GCAACTGTTCCTGAACTCAACT
RT-*IL-1β*-r	ATCTTTTGGGGTCCGTCAACT
Mutagenesis	
M-*scpA*5'-f	GGAACTGCAGCGCAAAGAAGAAAACTAAGCT
M-*scpA*3'-r	AATGGCAAGTTTATCAAATGG
M-*aad9NcoI*-f	CCATGGTCCTCGAGCTCTAGATCTTAAG
M-*aad9PstI*-r	CTGCAGGCGCTTACCAATTAGAATG
M-*scpA*3'-f	TAGACAATACGACGCCTGAAGC
M-*scpA*3'-r	ACCTGGTGTTTGACCTGAACTA
M-*silA*-f	CCCCAATCAGCTGCTTGAAGAT
M-*silA*-r	AACAAAGGAACGATGACATTG
M-*scpC*-f	CGCCATAATCCGTATGATTC
M-*scpC*-r	GACTGTTAAAAGGGATGATTTG
Verification	
V-*silA*5'-f	TTGCAGCAATGAATAGTG
V-*M13*-r	TGAAAAACGACGGCCAGT
V-*M13*-f	AACAGCTATGACCATGATTA
V-*silB*3'-r	TGAACCATTGACCTTTCGTC
V-*scpC*-f	ATCGCATCAATTTGCTTATGTC
V-*scpC*-r	GGCTGACCCACAGTGGATT
V-*sra*-f	CTGATGCTACTGCCAT
V-*sra*-r	GCGTTCAGGAAGTCTA

Table II. Bacterial strains and plasmids

Strain/plasmid	Relevant genotype/description	Reference
Strains		
E. coli		
JM109	F′ traD36 $proA^{+}B^{+}$ $lacI^{q}$ Δ(lacZ)M15/ Δ(lac-proAB) glnV44 $e14^{-}$ gyrA96 recA1 relA1 endA1 thi hsdR17 a cloning strain	Promega
GAS		
JS95	Wild type strain of serotype M14 isolated from a patient with NF	(Hidalgo-Grass *et al.*, 2002)}
silA^{-}	JS95 mutant with *silA* disruption created by pJ*silA*	This study
Δemm	JS95 mutant in which the M14 protein gene (*emm*) was replaced by Ω*km2* element	(Hidalgo-Grass *et al.*, 2002)
Δ*scpA*	JS95 mutant in which *scpA* was replaced by *aad9*	This study
Δ*scpA*/Δ*scpC*	JS95Δ*scpA*-derived mutant in which *scpC* was replaced by Ω*km2*	
Δ*scpA*/Δ*scpC*-pLZ	JS95Δ*scpA*/Δ*scpC* transformed with pLZ12 plasmid	This study
Δ*scpA*/Δ*scpC*-pL*scpC*	JS95Δ*scpA*/Δ*scpC* transformed with plZ12 plasmid harboring *scpC*	This study
Plasmids		
pGEM-T-Easy	A commercial T-vector	Promega
pG*scpC*	pGEM-T-easy harboring a 5313 bp DNA fragment containing *scpC*	This study
pUC4-21k	*E. coli* plasmid harboring the Ω*km2* element	(Perez-Casal *et al.*, 1991)
pG*scpC*Ω*km2*	pG*scpC* in which an *Eco*RV fragment was replaced with Ω*km* element	This study
pFW11	Streptococci-*E. coli* shuttle vector for genomic integration and allelic replacements harboring the *aad9* spectinomycin-resistance marker	(Podbielski *et al.*, 1996)
pJRS233	Streptococci-*E. coli* temperature sensitive shuttle vectors for genomic integration and allelic replacements harboring an erythromycin resistance marker	(Perez-Casal *et al.*, 1993)
pJ*scpAaad9*	pJRS233 containing 453 bp upstream of *scpA*, *aad9* and 486 bp of the 3' region of *scpA* and used for gene replacement	This study
pJ*silA*	pJRS233 containing a 492 bp internal fragment of *silA*	This study
pLZ12	Streptococci-*E. coli* shuttle vectors used for gene complementation harboring a kanamycin and chloramphenicol resistance markers	(Husmann *et al.*, 1995)
pL*scpC*	The pLZ12 vector containing *scpC* which was sub-cloned from pG*scpC*	This study

The serine peptidase families of GAS chosen for analysis of their transcription in the presence and absence of SilCR

Some of the chosen serine peptidases possess known protein targets, while others were homologues of bacterial peptidases with demonstrated virulence roles or phenotypic actions. S1C family member DegP (aka HtrA) plays a role in GAS biogenesis of streptolysin S and cysteine protease (Lyon and Caparon, 2004) and is homologous to peptidases which contribute to virulence in *Streptococcus pneumoniae* (Ibrahim *et al.*, 2004), and several Gram-negative pathogens (Cortes *et al.*, 2002; Elzer *et al.*, 1996; Johnson *et al.*, 1991; Purdy *et al.*, 2002). Family S8A is represented by two highly homologous peptidases, ScpA and the recently described SpyCEP (Edwards *et al.*, 2005) (for *S. pyogenes* cell envelope protease; SPy0416 in M1 genome). ScpA is known to cleave the C-terminus of human complement fragment C5a (anaphylotoxin), abolishing its capacity to bind PMN receptors and function as a chemokine (Cleary *et al.*, 1992b; Wexler *et al.*, 1985). SPy0416 is a homologue of the PrtS caseinases of *S. thermophilus, Lactococci* spp. and *Lactobacillus* spp. (Fernandez-Espla et al., 2000; Pritchard et al., 1994), as well as the group B *Streptococcus* (GBS) serine protease CspA, which cleaves fibrinogen and contributes to animal virulence (Harris *et al.*, 2003). The S9C and S15 (containing the *rbfA* and *pepXP* genes, respectively) are closely related families both involved in degradation of biologically active peptides, but without assigned function in GAS. Of note, S15 peptidases are homologous to mammalian dipeptidyl-peptidase IV that can remove dipeptides from the N-terminus of chemokines and cytokines (Van Damme *et al.*, 1999). Finally the S54 family is also unassigned in GAS, but the homologous AarA plays a role in population size-dependent regulation of gene expression in *Providencia stuartii* (Gallio and Kylsten, 2000).

Analysis of ScpC domains

To identify putative functional motifs of ScpC, we compared the amino acid (aa) sequences of ScpC and ScpA from eight available GAS genomes and from strain JS95 (GenBank accession numbers DQ192030), along with homologues sequences present in group B streptococcus (CspA) or *Lactococcus* and *Lactobacillus spp.* (PrtS). The comparison was conducted using multiple sequence alignments, secondary structure predictions and database homology searches (see "Materials and methods"), and revealed six putative functional domains in GAS ScpC (Figure 1B). The subtilisin-like proteases are translocated through the membrane via the signal sequence and finally are activated by cleavage of the pro-peptide domain (Siezen, 1999). The predicted cleavage site for the signal sequence is between Ala34 and Asp35, while the final processing site pre-pro-domain is between Val123 and Asn124. The peptidase region contains the catalytic triad of Asp + His + Ser located at residues 151, 279 and 617, respectively and the Asn381 which is predicted to be involved in formation of the oxyanion hole (Wilmouth et al. 2001). In cell envelope peptidases of *Lactococcus* and *Lactobacillus* spp., a distinction of the B and H domains has been offered along with a cooperative role of these domains in positioning the protease away from the bacterial cell surface (Siezen, 1999). As the border between the domains B and H in ScpC is not apparent, we have designated this domain B/H (Figure 1B).

Supplementary references

Cleary PP, Prahbu U, Dale JB, Wexler DE, Handley J. (1992). Streptococcal C5a peptidase is a highly specific endopeptidase. *Infect Immun* 60: 5219-5223.

Cortes G, de Astorza B, Benedi VJ, and Alberti S. (2002). Role of the *htrA* gene in *Klebsiella pneumoniae* virulence. *Infect Immun* 70: 4772-4776.

Edwards RJ, Taylor GW, Ferguson M, Murray S, Rendell N, Wrigley A, Bai Z, Boyle J, Finney SJ, Jones A, *et al.* (2005). Specific C-Terminal Cleavage and Inactivation of Interleukin-8 by Invasive Disease Isolates of *Streptococcus pyogenes*. *J Infect Dis* 192: 783-790.

Elzer PH, Phillips RW, Robertson GT, Roop RM, 2nd (1996). The HtrA stress response protease contributes to resistance of *Brucella abortus* to killing by murine phagocytes. *Infect Immun* 64: 4838-4841.

Fernandez-Espla MD, Garault P, Monnet V, Rul F. (2000) *Streptococcus thermophilus* cell wall-anchored proteinase: release, purification, and biochemical and genetic characterization. *Appl Environ Microbiol* 66: 4772-4778.

Gallio M, Kylsten P. (2000). *Providencia* may help find a function for a novel, widespread protein family. *Curr Biol* 10: R693-694.

Harris TO, Shelver DW, Bohnsack JF, Rubens CE. (2003). A novel streptococcal surface protease promotes virulence, resistance to opsonophagocytosis, and cleavage of human fibrinogen. *J Clin Invest* 111: 61-70.

Ibrahim YM, Kerr AR, McCluskey J, Mitchell TJ. (2004). Role of HtrA in the virulence and competence of *Streptococcus pneumoniae*. *Infect Immun* 72: 3584-3591.

Johnson K, Charles I, Dougan G, Pickard D, O'Gaora P, Costa G, Ali T, Miller I, Hormaeche C. (1991). The role of a stress-response protein in *Salmonella typhimurium* virulence. *Mol Microbiol* 5: 401-407.

Lyon WR, Caparon MG. (2004). Role for serine protease HtrA (DegP) of *Streptococcus pyogenes* in the biogenesis of virulence factors SpeB and the hemolysin streptolysin S. *Infect Immun* 72: 1618-1625.

Pritchard GG, Freebairn AD, Coolbear T. (1994). Purification and characterization of an endopeptidase from *Lactococcus lactis* subsp. cremoris SK11. *Microbiology* 140 (Pt 4): 923-930.

Purdy GE, Hong M, Payne SM. (2002). *Shigella flexneri* DegP facilitates IcsA surface expression and is required for efficient intercellular spread. *Infect Immun* 70: 6355-6364.

Van Damme J, Struyf S, Wuyts A, Van Coillie E, Menten P, Schols D, Sozzani S, De Meester I, Proost P. (1999). The role of CD26/DPP IV in chemokine processing. *Chem Immunol* 72: 42-56.

Wexler DE, Chenoweth DE, Cleary PP. (1985). Mechanism of action of the group A streptococcal C5a inactivator. *Proc Natl Acad Sci USA* 82: 8144-8148.

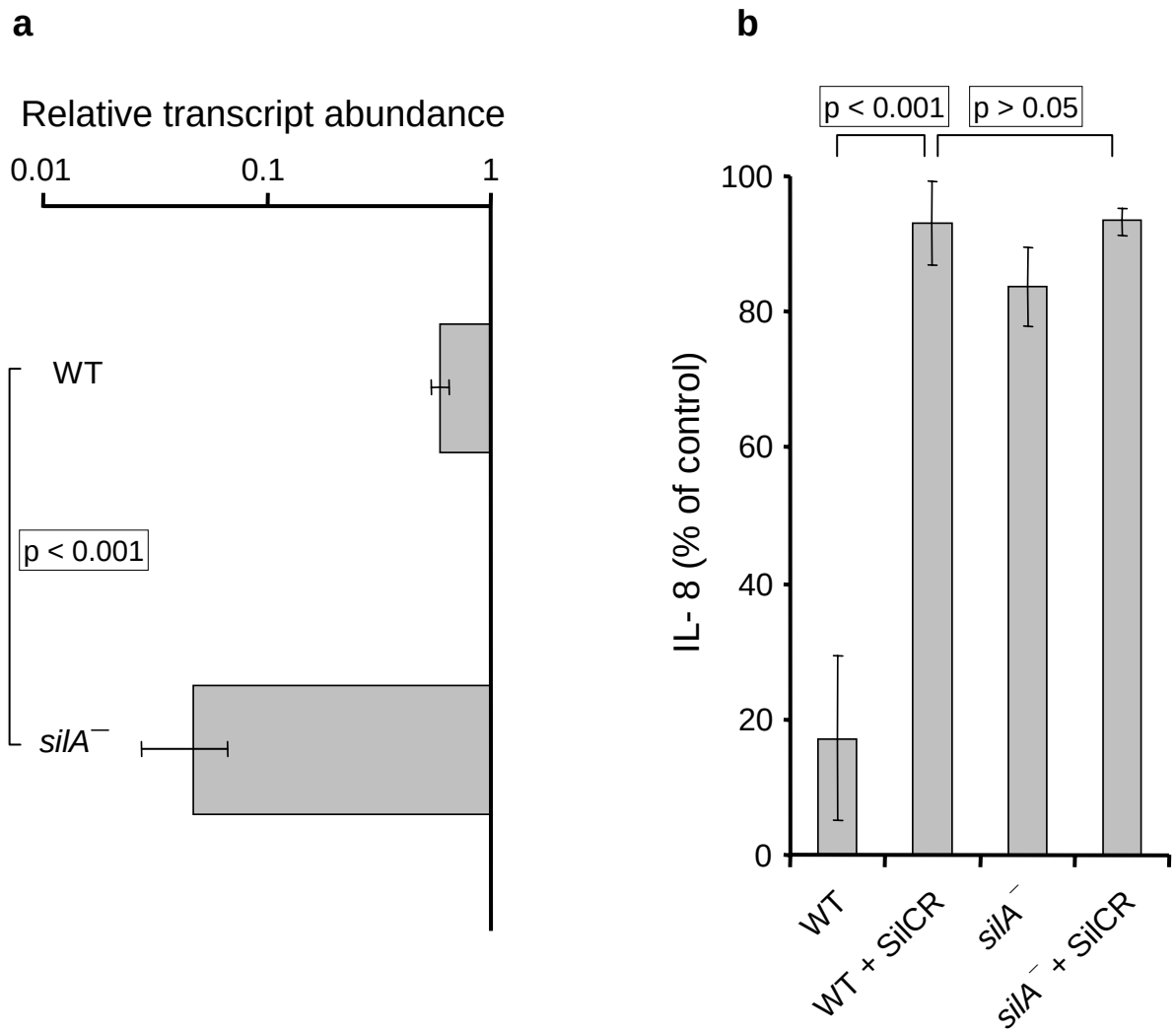

Figure 1S The transcription and expression of *scpC* is dependent on SilA/B. (**a**) The level of scpC transcription was significantly higher in the WT than in *silA*$^{-}$ ($p < 0.001$, student's test). The abundance of *scpC* transcripts relative to that of *gyrA* was determined by real-time RT-PCR on RNA derived from the WT and from the *silA*$^{-}$ mutant. Data shown are the amounts of transcript relative to that of *gyrA*. The values are mean obtained from analysis of triplicate of 3 independent RNA samples. Error bars represent SD. (**b**) SilA expression is required for the downregulation of IL-8 degradation in the presence of SilCR. The determination of IL-8 degradation by supernatants of WT and *silA*$^{-}$ mutant in absence and presence of SilCR (10 µg/ml) was conducted by ELISA. Control represents the IL-8 level in the in absence of bacterial supernatant, (100%) The values are mean obtained from analysis in duplicates of 3 independent experiments. Error bars represent SD. The degradation of IL-8 by WT supernatant is significantly higher $p < 0.001$ (student's test) than the degradation of IL-8 by the other supernatant samples.

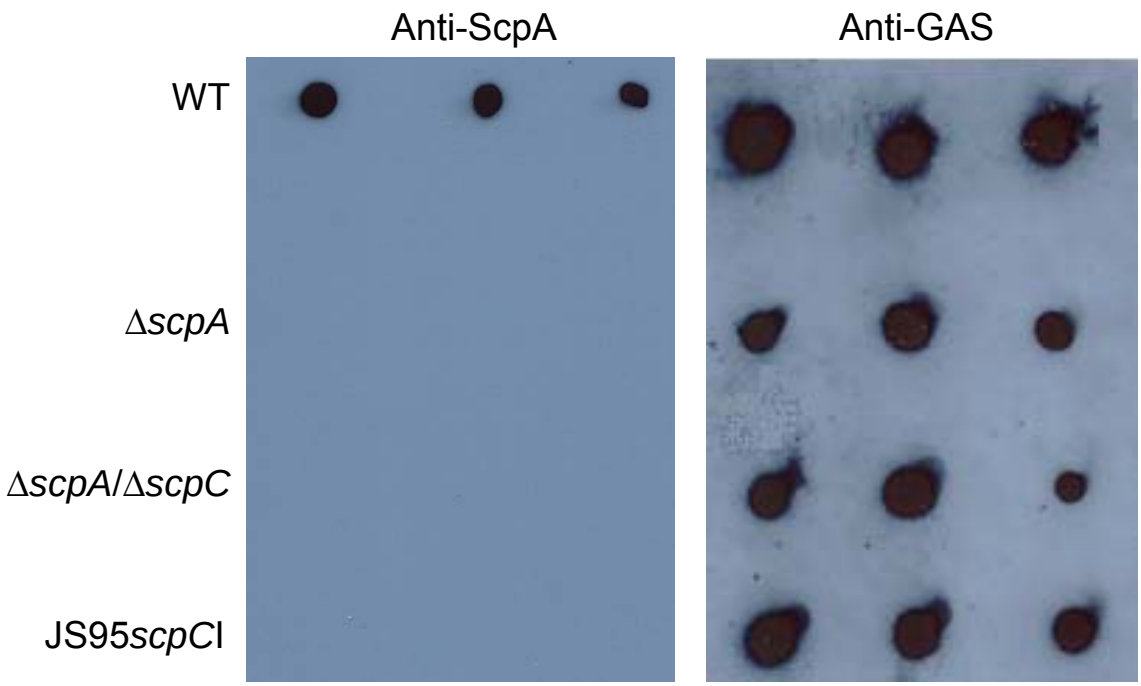

Figure 2S ScpA expression of various mutants. The expression of ScpA and of group A polysaccharide of GAS (as a control for bacterial number) was determined by dot blot assay on whole bacteria of WT and derived mutants (see Table II and Figure 4S).

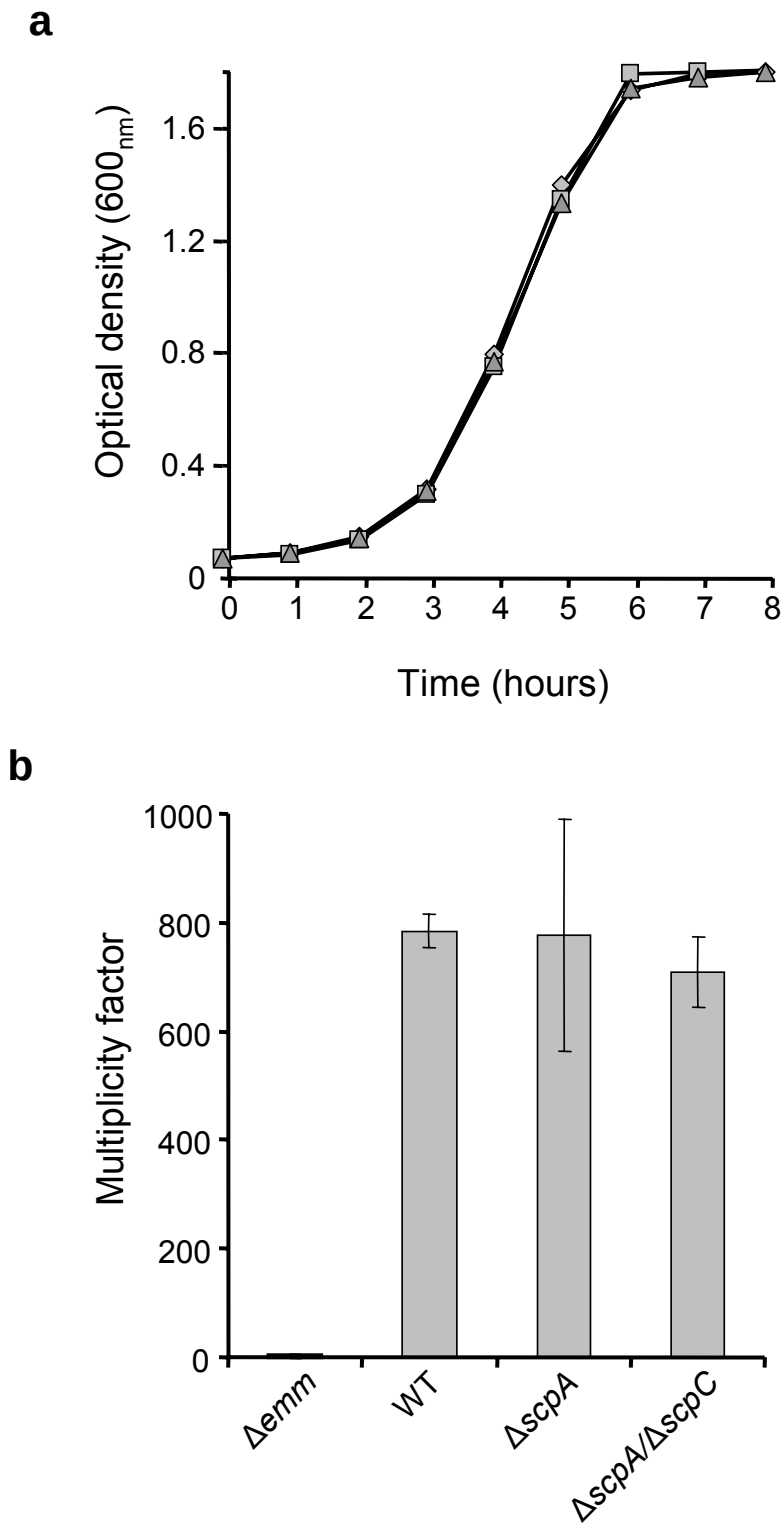

Figure 3S Growth comparison of WT and derived mutants in THY and in human blood. (**a**) Representative growth curves of WT (◆), Δ*scpA* (■), and Δ*scpA*/Δ*scpC* (▲) in THY at 37°C; readings of optical density were taken every hour at 600 nm. (**b**) WT and indicated mutants were added to non-immune human blood and the number of CFU after 3 hours of growth at 37°C was determined. Multiplicity factor (MF) was calculated by dividing the CFU of culture after 3 hours by the CFU of the original inoculums. The mean was calculated from the results of at least two separate experiments utilizing different donors. Error bars represent SD.

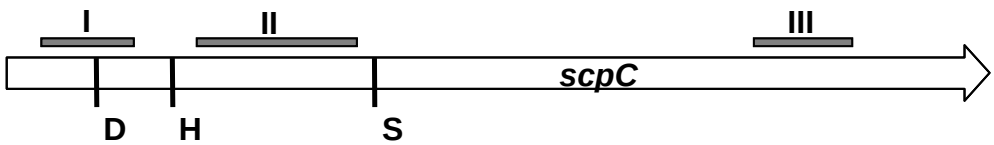

Figure 4S Different strategies used to inactivate *scpC* in WT JS95 background. To inactivate *scpC* in JS95 WT strain we cloned either fragments I or II of *scpC* into the pJRS233 vector. The resulting plasmids pJ*scpC*I and pJ*scpC*II were electroporated into JS95 and transformants resistant to erythromycin were selected at the non-permissive temperature of 37ºC. Only the transforments harboring pJ*scpC*I (JS95*scpC*I) lost their ability to degrade IL-8. Further analysis of JS95*scpC*I transformants showed that they also lost ScpA expression (see Figure 2S) due to insertion of fragment I into *scpA*. The scpC and scpA DNA fragments have position identity of 44.4%. In attempt to inactivate *scpC* by allelic replacement, we constructed an allele in which the *aad9* cassette was flanked upstream by fragment I, and downstream by fragment III (*Iaad9III*). The allele was cloned into pJRS233 to yield pJ*scpCIaad9III*. Neither transformation of JS95 by the linear allele nor with pJ*scpCIaad9III* resulted in *scpC* replacement.

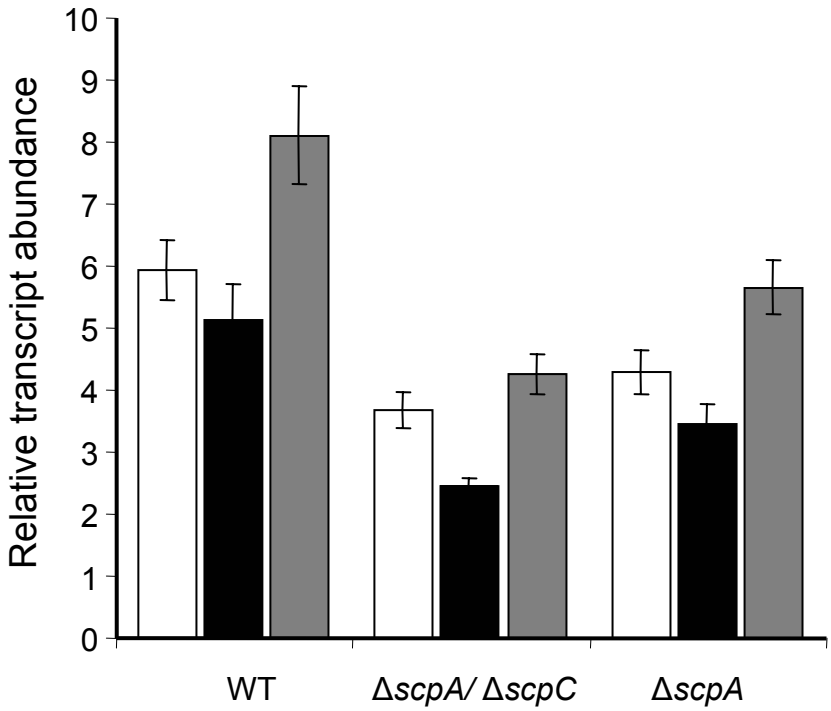

Figure 5S Induction of *KC, IL-1β, and IL-6* mRNA by WT and its derived mutants. Total RNA was prepared from lesional (GAS) and control (PBS) 6 mm punch biopsy specimens 24 hours after infection. The amount of each transcript was quantified by real time-RT-PCR and normalized to that of the housekeeping gene, *β1-actin*. Relative transcript abundance represents the level of expression of *KC* (empty bars), *IL-1β* (black bars), and *IL-6* (gray bars) in mice challenged with the indicated GAS strains compared to the corresponding genes expression level in mice challenged with PBS. The values are mean obtained from analysis of RNA prepared from 3 separate mice and the measurements were conducted in triplicates. Error bars represent SD.

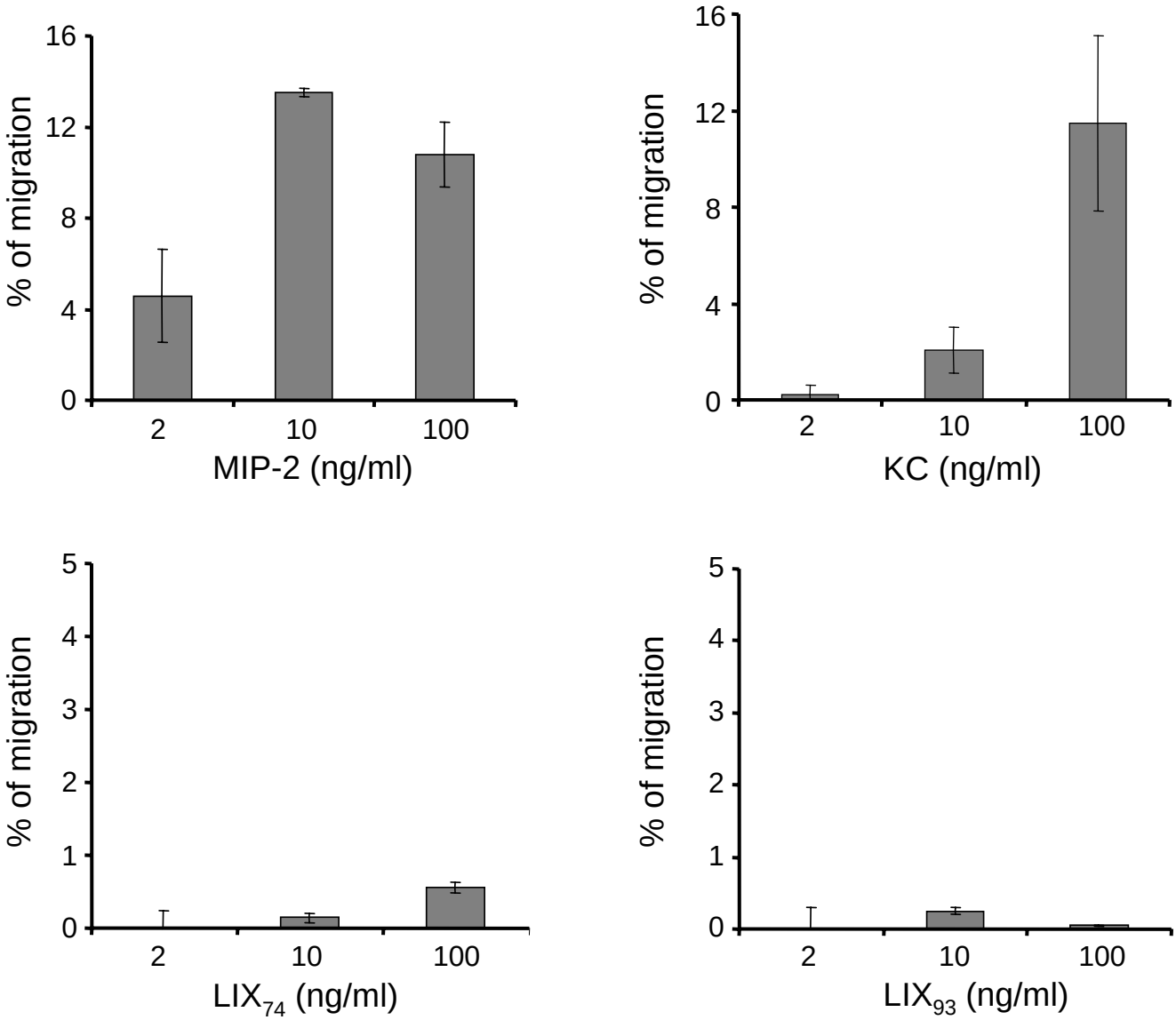

Figure 6S LIX has a marginal effect on murine PMN migration compared to that of either MIP-2 or KC. The ratio of migrating bone marrow-derived PMNs, across a trans-well into the lower chamber after exposure to the indicated concentrations of the designated chemokines, was performed as described in “Materials and methods”. The results shown represent the mean ratio ± SD of two independent determinations. The experiment was repeated twice yielding similar results.

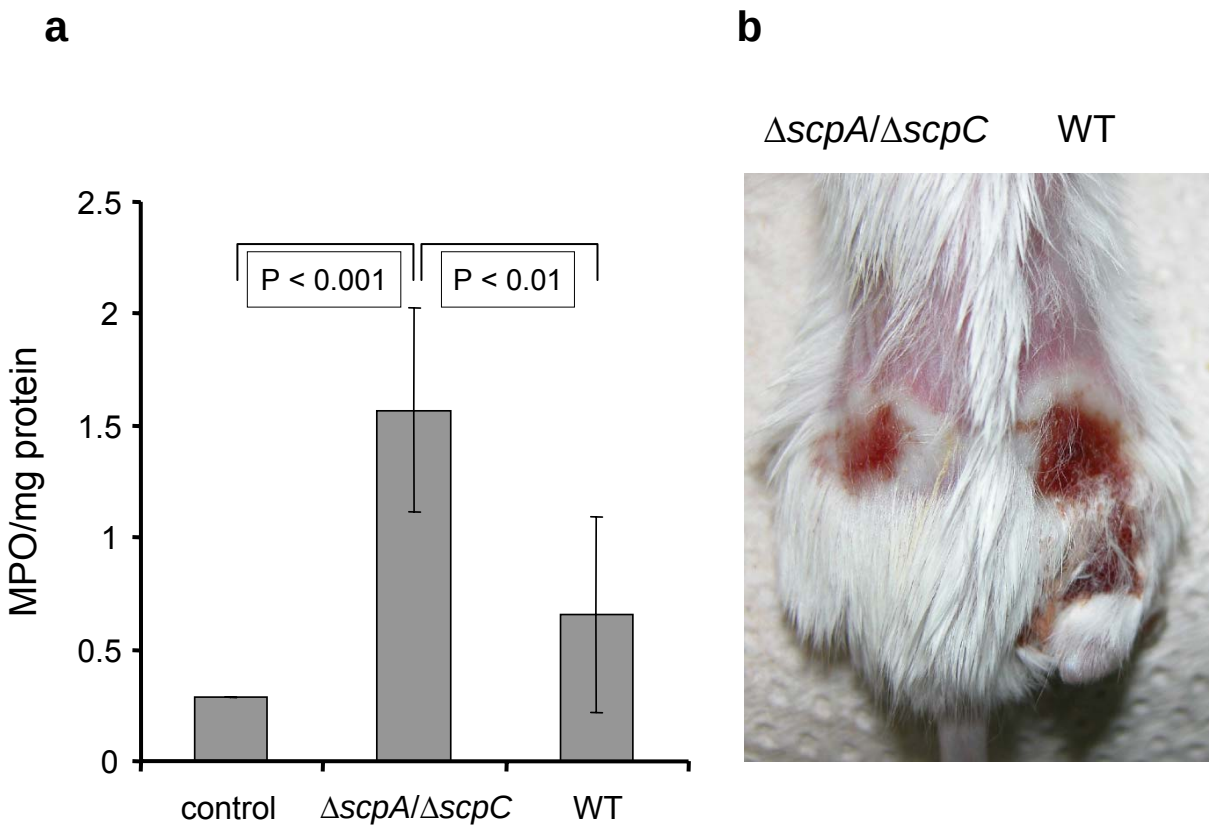

Figure 7S ScpC acts locally preventing PMN recruitment to the infection site. (**a**) Two groups of four mice were injected subcutaneously with 1 x 10^8 CFU of WT and with 1 x 10^8 CFU of Δ*scpA*/Δ*scpC* (which were administered into the opposite flanks of the same mouse) or with PBS. Forty eight hours after inoculation, lesional (GAS) and control (PBS) 6 mm punch biopsy specimens were taken and the amount of Myeloperoxidase (MPO) activity (units/mg protein) was determined. Each bar represents the mean ± SD of 2 determinations conducted on 4 specimens. $p < 0.01$ (student's test) of Δ*scpA*/Δ*scpC* versus WT. (**b**) A typical picture of a mouse 48 hours after challenge with Δ*scpA*/Δ*scpC* and with WT, administered at apposite flanks.